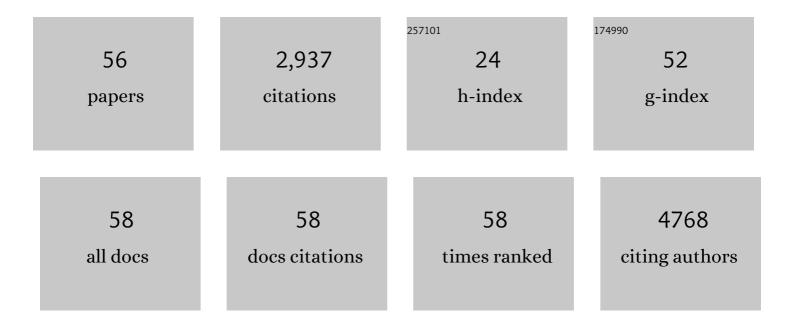
Mary C Scott

List of Publications by Year in descending order

Source: https://exaly.com/author-pdf/6961816/publications.pdf Version: 2024-02-01



| # | Article | IF | CITATIONS |
|----|---|------|-----------|
| 1 | Simultaneous Successive Twinning Captured by Atomic Electron Tomography. ACS Nano, 2022, 16, 588-596. | 7.3 | 12 |
| 2 | Chemical and Structural Alterations in the Amorphous Structure of Obsidian due to Nanolites. Microscopy and Microanalysis, 2022, 28, 289-295. | 0.2 | 4 |
| 3 | Orientated Growth of Ultrathin Tellurium by van der Waals Epitaxy. Advanced Materials Interfaces, 2022, 9, . | 1.9 | 7 |
| 4 | Automated Crystal Orientation Mapping in py4DSTEM using Sparse Correlation Matching. Microscopy and Microanalysis, 2022, 28, 390-403. | 0.2 | 17 |
| 5 | Thermodynamically Driven Synthetic Optimization for Cationâ€Disordered Rock Salt Cathodes. Advanced Energy Materials, 2022, 12, . | 10.2 | 20 |
| 6 | Structural heterogeneity in non-crystalline Te _{<i>x</i>} Se1â^'x thin films. Applied Physics Letters, 2022, 121, 012101. | 1.5 | 1 |
| 7 | Classifying handedness in chiral nanomaterials using label error robust deep learning. Npj Computational Materials, 2022, 8, . | 3.5 | 3 |
| 8 | 3D Nanotomography of calcium silicate hydrates by transmission electron microscopy. Journal of the American Ceramic Society, 2021, 104, 1852-1862. | 1.9 | 9 |
| 9 | Role of element-specific damping in ultrafast, helicity-independent, all-optical switching dynamics in amorphous (Gd,Tb)Co thin films. Physical Review B, 2021, 103, . | 1.1 | 40 |
| 10 | Understanding Diameter and Length Effects in a Solutionâ€Processable Telluriumâ€Poly(3,4â€Ethylenedioxythiophene) Polystyrene Sulfonate Hybrid Thermoelectric Nanowire Mesh. Advanced Electronic Materials, 2021, 7, 2000904. | 2.6 | 6 |
| 11 | Machine Learning Pipeline for Segmentation and Defect Identification from High-Resolution Transmission Electron Microscopy Data. Microscopy and Microanalysis, 2021, 27, 549-556. | 0.2 | 34 |
| 12 | Phase-contrast imaging of multiply-scattering extended objects at atomic resolution by reconstruction of the scattering matrix. Physical Review Research, 2021, 3, . | 1.3 | 11 |
| 13 | Decoupling electron and phonon transport in single-nanowire hybrid materials for high-performance thermoelectrics. Science Advances, 2021, 7, . | 4.7 | 30 |
| 14 | A layered nonstoichiometric lepidocrocite-type sodium titanate anode material for sodium-ion batteries. MRS Energy & Sustainability, 2021, 8, 88. | 1.3 | 4 |
| 15 | Tellurium Singleâ€Crystal Arrays by Lowâ€Temperature Evaporation and Crystallization. Advanced Materials, 2021, 33, e2100860. | 11.1 | 32 |
| 16 | A Fast Algorithm for Scanning Transmission Electron Microscopy Imaging and 4D-STEM Diffraction Simulations. Microscopy and Microanalysis, 2021, 27, 835-848. | 0.2 | 11 |
| 17 | Revealing the Phase Separation Behavior of Thermodynamically Immiscible Elements in a Nanoparticle. Nano Letters, 2021, 21, 6684-6689. | 4.5 | 18 |
| 18 | Structural Ordering and Composition of Warner Mountains Obsidian and its Microlites. Microscopy and Microanalysis, 2021, 27, 1850-1852. | 0.2 | 0 |

MARY C SCOTT

| # | Article | IF | CITATIONS |
|----|---|------|-----------|
| 19 | Prismatic 2.0 $\hat{a} \in$ Simulation software for scanning and high resolution transmission electron microscopy (STEM and HRTEM). Micron, 2021, 151, 103141. | 1.1 | 42 |
| 20 | Elucidating the local atomic and electronic structure of amorphous oxidized superconducting niobium films. Applied Physics Letters, 2021, 119, . | 1.5 | 10 |
| 21 | Evaporated tellurium thin films for p-type field-effect transistors and circuits. Nature Nanotechnology, 2020, 15, 53-58. | 15.6 | 153 |
| 22 | Tilted fluctuation electron microscopy. Applied Physics Letters, 2020, 117, . | 1.5 | 6 |
| 23 | Evaporated Se <i>_x</i> Te _{1â€} <i>_x</i> Thin Films with Tunable Bandgaps for Shortâ€Wave Infrared Photodetectors. Advanced Materials, 2020, 32, e2001329. | 11.1 | 49 |
| 24 | Characterization of mechanical degradation in an all-solid-state battery cathode. Journal of Materials Chemistry A, 2020, 8, 17399-17404. | 5.2 | 100 |
| 25 | Direct Bandgap-like Strong Photoluminescence from Twisted Multilayer MoS ₂ Grown on SrTiO ₃ . ACS Nano, 2020, 14, 16761-16769. | 7.3 | 16 |
| 26 | Direct Visualization of the Interfacial Degradation of Cathode Coatings in Solid State Batteries: A Combined Experimental and Computational Study. Advanced Energy Materials, 2020, 10, 1903778. | 10.2 | 67 |
| 27 | In-situ resonant band engineering of solution-processed semiconductors generates high performance n-type thermoelectric nano-inks. Nature Communications, 2020, 11, 2069. | 5.8 | 23 |
| 28 | Tilted Fluctuation Electron Microscopy Characterization of Magnetically Anisotropic Amorphous Metal Films. Microscopy and Microanalysis, 2019, 25, 1886-1887. | 0.2 | 0 |
| 29 | Machine Learning for High Throughput HRTEM Analysis. Microscopy and Microanalysis, 2019, 25, 150-151. | 0.2 | 7 |
| 30 | Engineering Chiral Structures Through Strain Release: Electron Tomography Study of Twisted Nanowires. Microscopy and Microanalysis, 2019, 25, 1804-1805. | 0.2 | 1 |
| 31 | Polaronic Trions at the MoS 2 /SrTiO 3 Interface. Advanced Materials, 2019, 31, 1903569. | 11.1 | 26 |
| 32 | Interface engineering for light-driven water oxidation: unravelling the passivating and catalytic mechanism in BiVO ₄ overlayers. Sustainable Energy and Fuels, 2019, 3, 127-135. | 2.5 | 28 |
| 33 | Helical van der Waals crystals with discretized Eshelby twist. Nature, 2019, 570, 358-362. | 13.7 | 91 |
| 34 | Optical and electrical properties of two-dimensional palladium diselenide. Applied Physics Letters, 2019, 114, . | 1.5 | 74 |
| 35 | Elimination of Response to Relative Humidity Changes in Chemical-Sensitive Field-Effect Transistors. ACS Sensors, 2019, 4, 1857-1863. | 4.0 | 24 |
| 36 | Ion Write Microthermotics: Programing Thermal Metamaterials at the Microscale. Nano Letters, 2019, 19, 3830-3837. | 4.5 | 45 |

MARY C SCOTT

| # | Article | IF | CITATIONS |
|----|---|----------|-----------|
| 37 | Synthetic WSe ₂ monolayers with high photoluminescence quantum yield. Science Advances, 2019, 5, eaau4728. | 4.7 | 78 |
| 38 | Three-dimensional Architecture Enabled by Strained Two-dimensional Material Heterojunction. Nano Letters, 2018, 18, 1819-1825. | 4.5 | 24 |
| 39 | Facile bottom-up synthesis of partially oxidized black phosphorus nanosheets as metal-free photocatalyst for hydrogen evolution. Proceedings of the National Academy of Sciences of the United States of America, 2018, 115, 4345-4350. | 3.3 | 207 |
| 40 | Linear and Nonlinear Reconstruction Algorithms for Atomic-Resolution Tomography Using Phase Contrast Electron Microscopy. Microscopy and Microanalysis, 2018, 24, 110-111. | 0.2 | 1 |
| 41 | Characterizing Magnetic Anisotropy in Amorphous Metal Films Using Tilted Fluctuation Electron Microscopy. Microscopy and Microanalysis, 2018, 24, 204-205. | 0.2 | 1 |
| 42 | Atomic Electron Tomography: Adding a New Dimension to See Single Atoms in Materials. Microscopy and Microanalysis, 2018, 24, 558-559. | 0.2 | 0 |
| 43 | Direct observation of anisotropic small-hole polarons in an orthorhombic structure of <mml:math xmlns:mml="http://www.w3.org/1998/Math/MathML"><mml:mrow><mml:mi>BiV</mml:mi><mml:msub><mml:m mathvariant="normal">O<mml:mn>4</mml:mn></mml:m></mml:msub></mml:mrow></mml:math> films. Physical Review B, 2018, 97. | i 1.1 | 7 |
| 44 | Solution-Synthesized High-Mobility Tellurium Nanoflakes for Short-Wave Infrared Photodetectors. ACS Nano, 2018, 12, 7253-7263. | 7.3 | 298 |
| 45 | Deciphering chemical order/disorder and material properties at the single-atom level. Nature, 2017, 542, 75-79. | 13.7 | 243 |
| 46 | Tunable and low-loss correlated plasmons in Mott-like insulating oxides. Nature Communications, 2017, 8, 15271. | 5.8 | 42 |
| 47 | Atomically Altered Hematite for Highly Efficient Perovskite Tandem Waterâ€Splitting Devices. ChemSusChem, 2017, 10, 2449-2456. | 3.6 | 71 |
| 48 | Efficient solar-driven electrochemical CO ₂ reduction to hydrocarbons and oxygenates. Energy and Environmental Science, 2017, 10, 2222-2230. | 15.6 | 145 |
| 49 | Nanomaterial datasets to advance tomography in scanning transmission electron microscopy. Scientific Data, 2016, 3, 160041. | 2.4 | 42 |
| 50 | Three-Dimensional Determination of the Coordinates of Individual Atoms in Materials. Microscopy and Microanalysis, 2016, 22, 916-917. | 0.2 | 0 |
| 51 | Stability Studies of MAPbI 3 : Identification of Degradation Pathways and Strategies for Observing the Native Structure of Lead Halide Perovskites. Microscopy and Microanalysis, 2016, 22, 1510-1511. | 0.2 | 1 |
| 52 | Three-dimensional coordinates of individual atoms in materials revealed by electronÂtomography. Nature Materials, 2015, 14, 1099-1103. | 13.3 | 172 |
| 53 | Three-Dimensional Imaging of Dislocations and Defects in Materials at Atomic Resolution Using Electron Tomography. Microscopy and Microanalysis, 2014, 20, 1062-1063. | 0.2 | 0 |
| 54 | Atomic Resolution Tomography of Magnetically Anisotropic FePt Nanoparticles. Microscopy and Microanalysis, 2014, 20, 804-805. | 0.2 | 1 |

| # | Article | IF | CITATIONS |
|----|---|------|-----------|
| 55 | Towards three-dimensional structural determination of amorphous materials at atomic resolution. Physical Review B, 2013, 88, . | 1.1 | 17 |
| 56 | Electron tomography at 2.4-ångström resolution. Nature, 2012, 483, 444-447. | 13.7 | 366 |